2024 IEEE 63rd Conference on Decision and Control (CDC)
December 16-19, 2024. MiCo, Milan, Italy

Enhanced Battery State Estimation: Part 1 – Electrolyte Lithium-ion Concentration Observer

Sara Sepasiahooyi and Shu-Xia Tang

2024 IEEE 63rd Conference on Decision and Control (CDC) | 979-8-3503-1633-9/24/$31.00 ©2024 IEEE | DOI: 10.1109/CDC56724.2024.10885885

***Abstract*— This paper introduces backstepping closed-loop observers designed to estimate the concentration of lithium ions in the electrolyte within the negative electrode, positive electrode, and separator. The battery model employed is the Single Particle Model with electrolyte (SPMe) dynamics. Partial Differential Equation (PDE) backstepping observers are proposed to estimate electrolyte lithium concentration in the negative and positive electrodes, followed by a separator observer based on these results. The electrolyte lithium concentration observers for the positive and negative electrodes require the concentration at the boundaries. As direct measurement of this concentration is challenging, an alternative measurable parameter will be identified for indirect calculation. While Part 1 of this study operates independently, Part 2 complements it by conducting reverse sensitivity analysis to determine the most appropriate measurable parameter. The convergence of the estimation error for the designed observers is ensured through Lyapunov stability analysis. A simulation on a $LiFePO_4$ battery cell under an Urban Dynamometer Driving Schedule (UDDS) current profile is included to confirm the theoretical aspects and the convergence of the state estimation error.**

***Index Terms*— Li-ion battery; State estimation; Electrolyte concentration; SPMe; Backstepping observer.**

I. Introduction

In the field of lithium-ion batteries, electrolyte lithium concentration is considered one of the most significant State-of-Health indicators, as the battery's voltage is highly sensitive to this parameter [1]. Information about the concentration of lithium ions in the electrolyte is valuable for predicting battery behavior [2]. However, measuring this parameter is challenging. Therefore, accurate estimation of electrolyte concentration at every time and position becomes crucial. In recent years, the literature on battery state estimation has expanded significantly. Studies on battery state estimation can be broadly classified into data-driven methods [3] and model-based methods. The model-based category encompasses electrochemical models and equivalent circuit models [4]. Electrochemical models offer precise predictions of internal state variables. Observers for solid phase lithium-ion concentration are designed in [5], and these observers are improved by considering temperature variation effects and integrating thermal dynamics into the battery model [6]. Moura et al. [7] propose observers for lithium concentration in the solid phase and open-loop observers for lithium concentration in the electrolyte phase. In this paper, we propose closed-loop PDE observers for the negative and positive electrodes, followed by a separator observer employing a backstepping approach. These are cascaded observers, as the required measurements for the separator observer are derived from the electrolyte lithium concentration observers in either the negative or positive electrodes. The designed observers require the concentration at the boundaries. Due to the complexity of measuring lithium concentration, an alternative measurable parameter is required to calculate the lithium concentration at the boundaries. In Part 2 of this study [8], reverse sensitivity analysis is conducted to identify the most appropriate measurable parameter. The main contributions of this study are as follows:

- In [7], open-loop observers were designed for electrolyte lithium concentration. However, to the best of our knowledge, this study is the first to introduce closed-loop observers for electrolyte lithium concentration, utilizing state estimation errors at the boundaries between the electrodes and current collectors.
- In this study, SPMe is employed to provide a more accurate battery model by incorporating electrolyte dynamics, particularly at high C-rates.
- Unlike [9], which discretizes concentration states, this work designs observers that operate directly on the PDEs without relying on discretization.
- The modified boundary conditions at the electrode/separator interfaces simplify the solution process of PDEs and facilitate the formulation of observers. To the best of the author's knowledge, this is the first time modified boundary conditions have been used in observer design.

The rest of this document is structured as follows: Section II introduces the battery model. The proposed observers for negative electrode, positive electrode and separator are detailed in Section III, with the simulation results presented in Section IV. Finally, Section V provides the conclusions and outlines future work.

II. Electrolyte dynamics in SPMe

In this section, the SPMe is illustrated in Fig. 1, and the PDEs for electrolyte lithium concentration, and modified boundary conditions and the availability of the model's states at the terminal boundaries, are explained in detail.

A. Electrolyte concentration

The electrolyte lithium concentration within the negative electrode $c_e^-(t,x)$, along with the boundary conditions, is

S. Sepasiahooyi and S.-X. Tang (correspondening author) are with the Department of Mechanical Engineering, Texas Tech University, Lubbock, USA. ssepasia@ttu.edu, shuxia.tang@ttu.edu.

Authorized licensed use limited to: Texas Tech University. Downloaded on March 19,2025 at 15:08:22 UTC from IEEE Xplore. Restrictions apply.

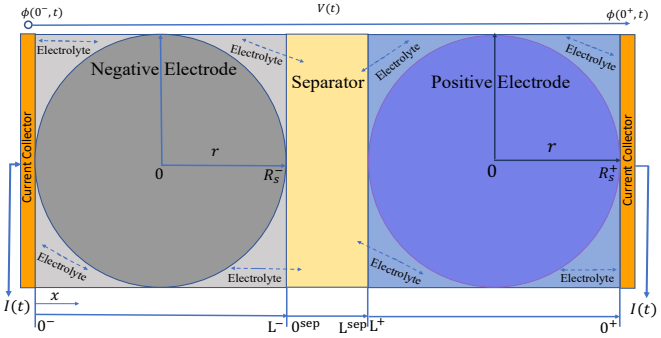

Fig. 1: Schematic of SPMe

given by:

$$\frac{\partial c_e^-}{\partial t}(t,x) = \frac{\partial}{\partial x}\left[\frac{D_e^{-,\text{eff}}(c_e^-(t,x))}{\varepsilon_e^-}\frac{\partial c_e^-}{\partial x}(t,x)\right] + \frac{(1-t_c^0)}{\varepsilon_e^- F L^-} I(t) \tag{II.1}$$

$$\frac{\partial c_e^-}{\partial x}(t,0^-) = 0, \tag{II.2}$$

$$D_e^{-,\text{eff}}(c_e^-(t,x))\frac{\partial c_e^-(t,L^-)}{\partial x} = D_e^{\text{sep,eff}}(c_e^-(t,x))\frac{\partial c_e^{\text{sep}}(t,0^{\text{sep}})}{\partial x} \tag{II.5}$$

To simplify the design of observers, the following assumption in the model is considered:

Assumption 1. *Effective electrolyte diffusivity, $D_e^{i,eff}(c_e^i(t,x)), i \in \{-, sep, +\}$, remains constant.*

Note that in Part 2 [8], the complexity of this parameter is maintained. Electrolyte lithium concentration in the positive electrode $c_e^+(t,x)$, and the boundary conditions are given by:

$$\frac{\partial c_e^+}{\partial t}(t,x) = \frac{\partial}{\partial x}\left[\frac{D_e^{+,\text{eff}}}{\varepsilon_e^+}\frac{\partial c_e^+}{\partial x}(t,x)\right] - \frac{(1-t_c^0)}{\varepsilon_e^+ F L^+} I(t), \tag{II.3}$$

$$\frac{\partial c_e^+}{\partial x}(t,0^+) = 0, \tag{II.4}$$

$$D_e^{+,\text{eff}}\frac{\partial c_e^+}{\partial x}(t,L^+) = D_e^{\text{sep,eff}}\frac{\partial c_e^{\text{sep}}(t,L^{\text{sep}})}{\partial x}. \tag{II.5}$$

The electrolyte lithium concentration in the separator $c_e^{\text{sep}}(t,x)$, and the boundary conditions are expressed as:

$$\frac{\partial c_e^{\text{sep}}}{\partial t}(t,x) = \frac{\partial}{\partial x}\left[\frac{D_e^{\text{sep,eff}}}{\varepsilon_e^{\text{sep}}}\frac{\partial c_e^{\text{sep}}}{\partial x}(t,x)\right], \tag{II.6}$$

$$D_e^{\text{sep,eff}}\frac{\partial c_e^{\text{sep}}}{\partial x}(t,0^{\text{sep}}) = D_e^{-,\text{eff}}\frac{\partial c_e^-}{\partial x}(t,L^-), \tag{II.7}$$

$$D_e^{\text{sep,eff}}\frac{\partial c_e^{\text{sep}}}{\partial x}(t,L^{\text{sep}}) = D_e^{+,\text{eff}}\frac{\partial c_e^+}{\partial x}(t,L^+), \tag{II.8}$$

$$c_e^i(0,x) = c_{e,0}^i(x), i \in \{-,\text{sep},+\}, \tag{II.9}$$

where ε_e^i, and L^i, $i \in \{-,\text{sep},+\}$, represent the volume fraction of the electrolyte, and the thickness of the battery regions, respectively. t_c^0 is the transference number. $I(t)$ denotes the battery current as the input to the model, and F is Faraday's constant. $c_{e,0}^i(x)$ represents the initial conditions, which afterward have been omitted from the equations for simplicity but are considered in the full analysis.

The electrolyte concentration PDEs in (II.1), (II.3), and (II.6) have coupled boundary conditions. To handle the interconnected electrolyte PDEs, all six coupled boundary conditions must be applied together. This scenario complicates the system significantly in terms of solving the PDEs. To facilitate the solution process and enable the design of observers, non-coupled modified boundary conditions are introduced in the next section.

B. Modified boundary conditions

To establish the modified boundary conditions, the following assumption and the equilibrium point P^* within the separator domain are considered, as depicted in Fig. 2.

Assumption 2. *The overall quantity of lithium moles in the electrolyte $n_{Li,e}$ and solid phase $n_{Li,s}$ remains constant.*

Assumption 3. *The electrode current density $i_s^{\pm}(t,x)$ and electrolyte current density $i_e^{\pm}(t,x)$ are approximated by their average values $\bar{i}_s^{\pm}(t)$ and $\bar{i}_e^{\pm}(t)$.*

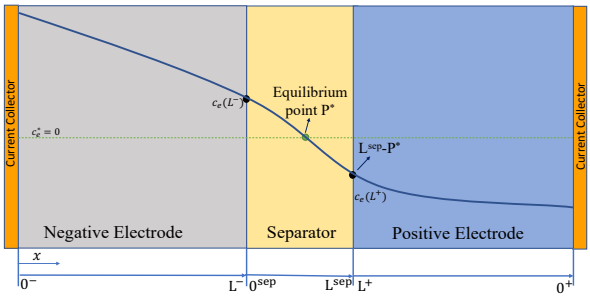

Fig. 2: Modified boundary condition for electrolyte concentration

Based on Assumption 2, the mass conversion of electrolyte lithium ions at the equilibrium point P^* is described as [10]:

$$\frac{\bar{i}_e^-(t)+\bar{i}_s^-(t)}{F}L^- + \frac{\bar{i}_e^{\text{sep}}(t)}{F}P^* = \frac{\bar{i}_e^{\text{sep}}(t)}{F}(L^{\text{sep}}-P^*) + \frac{\bar{i}_e^+(t)+\bar{i}_s^+(t)}{F}L^+. \tag{II.10}$$

Although the electrode current density and the electrolyte current density vary at each point inside the battery, based on Assumption 3, the total current density is expressed as follows [10]:

$$\bar{i}_e^{\pm}(t) + \bar{i}_s^{\pm}(t) = \frac{I(t)}{A}, \bar{i}_e^{\text{sep}}(t) = \frac{I(t)}{A}, \tag{II.11}$$

where A is the electrode surface area. By solving (II.10) through (II.11), the equilibrium point position can be obtained as:

$$P^* = \frac{L^{\text{sep}} + L^+ - L^-}{2}. \tag{II.12}$$

The electrolyte concentration behavior in the separator is assumed to be quasi-linear. Quasi-linear behavior implies that, despite some nonlinearities, the relationship between

Authorized licensed use limited to: Texas Tech University. Downloaded on March 19,2025 at 15:08:22 UTC from IEEE Xplore. Restrictions apply.

lithium concentration and position in the separator can be approximated as linear within the domain of interest. Assuming quasi-linear behavior of lithium concentration in the separator domain, $\frac{\partial c_e^-}{\partial x}(t, L^-)$ can be interpreted as the slope of a line in the separator region. By setting the electrolyte concentration at the equilibrium point to zero, the modified boundary condition for the negative electrode/separator interface is formulated as follows [10]:

$$\frac{\partial c_e^-}{\partial x}(t, L^-) = \frac{-c_e^-(t, L^-)}{P^*}.$$

Similarly, the modified boundary condition at the positive electrode/separator interface is given in [10]:

$$\frac{\partial c_e^+}{\partial x}(t, L^+) = \frac{c_e^+(t, L^+)}{L^{\text{sep}} - P^*}.$$

C. Availability of electrolyte lithium concentration at the terminal boundaries $c_e^{\pm}(t, 0^{\pm})$

For the design of the proposed electrolyte lithium concentration observers in the negative and positive electrodes, knowledge of the electrolyte lithium concentration at the terminal boundaries $c_e^{\pm}(t, 0^{\pm})$, is required. Given the difficulty of directly measuring this parameter, a related measurable parameter is used to obtain $c_e^{\pm}(t, 0^{\pm})$. In Part 2 [8], an inverse sensitivity analysis of the electrolyte lithium concentration at the terminal boundaries $c_e^{\pm}(t, 0^{\pm})$ is conducted to three measurable parameters: electrolyte conductivity, electrolyte diffusion coefficient, and electrolyte resistance. An analytical derivation was performed as a sensitivity method, which is a versatile approach applicable to various battery materials. This study stands alone; However, to delve deeper, Part 2 [8] identified electrolyte resistance as the most suitable measurement in $LiFePO_4$ battery cell for obtaining the required electrolyte concentration at the boundaries. Electrolyte resistance at the boundaries can be measured by Electrochemical Impedance Spectroscopy (EIS).

Remark 1. Note that this scheme requires EIS, which is an offline method. Typically, an EIS spectrum, consisting of measurements at 60 frequencies ranging from 100 kHz to 0.1 Hz, takes about 2 to 3 minutes to complete [11]. Integrating the event-triggered approach [12] into the observer is a potential area for future work.

III. Observer design

A. Normalization of system

To simplify the design of the observer system, normalization is applied. Let $\bar{x} = \frac{x}{L^{\pm}}$ and $\bar{t} = \frac{D_e^{\pm,\text{eff}}}{(L^{\pm})^2 \varepsilon_e^{\pm}} t$. Henceforth, the bars over the space and time coordinates are removed to simplify notation. The normalized electrolyte lithium concentration within the negative electrode, along with its boundary conditions, is presented as follows:

$$\frac{\partial c_{\text{e}}^-(t,x)}{\partial t} = \frac{\partial^2 c_{\text{e}}^-(t,x)}{\partial x^2} + \frac{L^-(1-t_c^0)}{D_{\text{e}}^{-,\text{eff}} F} I(t), \tag{III.1}$$

$$\frac{\partial c_{\text{e}}^-}{\partial x}(t, 0^-) = 0, \tag{III.2}$$

$$\frac{\partial c_e^-}{\partial x}(t, 1^-) = \frac{-L^- c_e^-(t, 1^-)}{P^*}, \tag{III.3}$$

where $t > 0$ and $x \in (0, 1)$. The normalized electrolyte lithium concentration in the positive electrode and its boundary conditions are as follows:

$$\frac{\partial c_{\text{e}}^+(t,x)}{\partial t} = \frac{\partial^2 c_{\text{e}}^+(t,x)}{\partial x^2} - \frac{L^+(1-t_c^0)}{D_{\text{e}}^{+,\text{eff}} F} I(t), \tag{III.4}$$

$$\frac{\partial c_{\text{e}}^+}{\partial x}(t, 0^+) = 0, \tag{III.5}$$

$$\frac{\partial c_e^+}{\partial x}(t, 1^+) = \frac{L^+ c_e^+(t, 1^+)}{L^{\text{sep}} - P^*}. \tag{III.6}$$

The normalized electrolyte lithium concentration in the separator and boundary conditions are as follows:

$$\frac{\partial c_{\text{e}}^{\text{sep}}(t,x)}{\partial t} = \frac{\partial^2 c_{\text{e}}^{\text{sep}}(t,x)}{\partial x^2}, \tag{III.7}$$

$$\frac{\partial c_{\text{e}}^{\text{sep}}}{\partial x}(t, 0^{\text{sep}}) = \frac{-L^- c_e^{\text{sep}}(t, 0^{\text{sep}})}{P^*}, \tag{III.8}$$

$$\frac{\partial c_e^{\text{sep}}}{\partial x}(t, 1^{\text{sep}}) = \frac{L^+ c_e^{\text{sep}}(t, 1^{\text{sep}})}{L^{\text{sep}} - P^*}. \tag{III.9}$$

B. Electrolyte observer for negative electrode

The proposed observer for the normalized electrolyte lithium concentration in the negative electrode (III.1)-(III.3) is designed as follows. The hat notation $\hat{}$ above a parameter denotes its estimated value.

$$\frac{\partial \hat{c}_{\text{e}}^-}{\partial t}(t,x) = \frac{\partial^2 \hat{c}_{\text{e}}^-}{\partial x^2}(t,x) + \frac{L^-(1-t_c^0)}{D_{\text{e}}^{-,\text{eff}} F} I(t) + p_1(x)(c_{\text{e}}^-(t,0^-) - \hat{c}_{\text{e}}^-(t,0^-)), \tag{III.10}$$

$$\frac{\partial \hat{c}_{\text{e}}^-}{\partial x}(t, 0^-) = p_{10}(c_{\text{e}}^-(t,0^-) - \hat{c}_{\text{e}}^-(t,0^-)), \tag{III.11}$$

$$\frac{\partial \hat{c}_{\text{e}}^-}{\partial x}(t, 1^-) = \frac{-L^- \hat{c}_{\text{e}}^-(t, 1^-)}{P^*}, \tag{III.12}$$

where $p_1(x)$ and p_{10} are the observer gains. The observer gains will be determined such that $\hat{c}_{\text{e}}^-(t,x)$ converges to $c_{\text{e}}^-(t,x)$ as time approaches infinity. The dynamic of the state estimation error $\tilde{c}_e^-(t,x) = c_e^-(t,x) - \hat{c}_e^-(t,x)$ is obtained as:

$$\frac{\partial \tilde{c}_{\text{e}}^-}{\partial t}(t,x) = \frac{\partial^2 \tilde{c}_{\text{e}}^-}{\partial x^2}(t,x) + p_1(x)\tilde{c}_{\text{e}}^-(t,0^-), \tag{III.13}$$

$$\frac{\partial \tilde{c}_{\text{e}}^-}{\partial x}(t, 0) = -p_{10}\tilde{c}_{\text{e}}^-(t,0^-), \tag{III.14}$$

$$\frac{\partial \tilde{c}_{\text{e}}^-}{\partial x}(t, 1^-) = \frac{-L^- \tilde{c}_{\text{e}}^-(t, 1^-)}{P^*}. \tag{III.15}$$

By finding the following invertible transformation:

$$\tilde{c}_e^-(t,x) = \tilde{w}(t,x) - \int_0^x p(x,y)\tilde{w}(t,y)dy, \tag{III.16}$$

Authorized licensed use limited to: Texas Tech University. Downloaded on March 19,2025 at 15:08:22 UTC from IEEE Xplore. Restrictions apply.

the error system (III.13)-(III.15) will be transformed into the exponentially stable target system as follows:

$$\frac{\partial \tilde{w}}{\partial t}(t,x) = \frac{\partial^2 \tilde{w}}{\partial x^2}(t,x) - \lambda \tilde{w}(t,x), \tag{III.17}$$

$$\frac{\partial \tilde{w}}{\partial x}(t,0) = 0, \tag{III.18}$$

$$\frac{\partial \tilde{w}}{\partial x}(t,1^-) = -q^- \tilde{w}(t,1^-), \tag{III.19}$$

where $q^- = \frac{L^-}{P^*}$. $\lambda \geq -\frac{1}{4}$ is an arbitrarily chosen parameter that determines the convergence rate of the proposed observer to the system states. By differentiating transformation (III.16) with respect to t and twice with respect to x, and then equating their difference to satisfy (III.13), the following kernel function PDE is obtained:

$$\frac{\partial^2 P}{\partial x^2}(x,y) - \frac{\partial^2 P}{\partial y^2}(x,y) = -\lambda P(x,y), \tag{III.20}$$

$$\frac{\partial P}{\partial x}(1,y) = -q^- P(1,y), \tag{III.21}$$

$$P(x,x) = -\frac{\lambda}{2}x. \tag{III.22}$$

The solution of the kernel function PDE (III.20)-(III.22) is achieved as follows (eq. 7 in [13]):

$$\begin{aligned} P(x,y) =& \frac{-\lambda q^-}{\sqrt{\lambda + (q^-)^2}} \\ & \times \int_0^{x-y} e^{q^-\tau/2} I_0\left(\sqrt{\lambda(2-x-y)(x-y-\tau)}\right) \\ & \times \sinh\left(\frac{\sqrt{\lambda+(q^-)^2}}{2}\tau\right) d\tau \\ & - \lambda(1-y)\frac{I_1\left(\sqrt{\lambda\left((1-y)^2-(1-x)^2\right)}\right)}{\sqrt{\lambda\left((1-y)^2-(1-x)^2\right)}}, \end{aligned} \tag{III.23}$$

where $I_m(.)$ represents the modified Bessel functions of the first kind. The observer gains $p_1(x)$ and p_{10} are obtained as follows:

$$p_1(x) = -P_y(x,0), \tag{III.24}$$

$$p_{10} = -\frac{\lambda}{2}. \tag{III.25}$$

Theorem 1. Consider the normalized system for the negative electrode (III.1)-(III.3) and proposed state observer (III.10)-(III.12) with its gains (III.24) and (III.25). For any initial condition under assumptions, if $\lambda \geq -\frac{1}{4}$, then the origin of the error system (III.13)-(III.15) is exponentially stable. This implies that the designed observer (III.10)-(III.12) converges exponentially to the system (III.1)-(III.3).

Proof: Considering the Lyapunov function $V(t) = \frac{1}{2}\left\|\tilde{w}(t,\cdot)\right\|_{L_2}^2$, and using the approach in [6], $\dot{V}(t)$ is negative semi-definite if $\geq -\frac{1}{4}$. Hence, the target system is exponentially stable. Given the invertibility of the transformation (III.16), it can be concluded that the state estimation error in (III.13)-(III.15) is also exponentially stable.

C. Electrolyte observer for positive electrode

An observer for the normalized electrolyte lithium concentration in the positive electrode, as described in (III.4), (III.5), and (III.6), is proposed as follows:

$$\begin{aligned} \frac{\partial \hat{c}_{\mathrm{e}}^+}{\partial t}(t,x) =& \frac{\partial^2 \hat{c}_{\mathrm{e}}^+}{\partial x^2}(t,x) - \frac{L^+(1-t_c^0)}{D_{\mathrm{e}}^{+,\mathrm{eff}}F} I(t) \\ & + p_1(x)(c_{\mathrm{e}}^+(t,0^+) - \hat{c}_{\mathrm{e}}^+(t,0^+)), \end{aligned} \tag{III.26}$$

$$\frac{\partial \hat{c}_{\mathrm{e}}^+}{\partial x}(t,0^+) = p_{10}(c_{\mathrm{e}}^+(t,0^+) - \hat{c}_{\mathrm{e}}^+(t,0^+)), \tag{III.27}$$

$$\frac{\partial \hat{c}_{\mathrm{e}}^+}{\partial x}(t,1^+) = \frac{L^+ \hat{c}_{\mathrm{e}}^+(t,1^+)}{L^{\mathrm{sep}} - P^*}, \tag{III.28}$$

where $p_1(x)$ and $p_{10}(x)$ are designed as in (III.24) and (III.25), with q^- replaced by $q^+ = \frac{-L^+}{L^{\mathrm{sep}}-P^*}$ in (III.23). The state estimation error $\tilde{c}_{\mathrm{e}}^+(t,x) = c_{\mathrm{e}}^+(t,x) - \hat{c}_{\mathrm{e}}^+(t,x)$ system in the positive electrode is described as follows:

$$\frac{\partial \tilde{c}_{\mathrm{e}}^+}{\partial t}(t,x) = \frac{\partial^2 \tilde{c}_{\mathrm{e}}^+}{\partial x^2}(t,x) + p_1(x)\tilde{c}_{\mathrm{e}}^+(t,0^+), \tag{III.29}$$

$$\frac{\partial \tilde{c}_{\mathrm{e}}^+}{\partial x}(t,0) = -p_{10}\tilde{c}_{\mathrm{e}}^+(t,0^+), \tag{III.30}$$

$$\frac{\partial \tilde{c}_{\mathrm{e}}^+}{\partial x}(t,1^+) = \frac{L^+ \tilde{c}_{\mathrm{e}}^+(t,1^+)}{L^{\mathrm{sep}} - P^*}. \tag{III.31}$$

Then, with the following invertible transformation:

$$\tilde{c}_{\mathrm{e}}^+(t,x) = \tilde{w}(t,x) - \int_0^x p(x,y)\tilde{w}(t,y)dy, \tag{III.32}$$

the error system (III.29)-(III.31) will be transformed into the an exponentially stable target system $\tilde{w}(t,x)$ with replacing q^+ with q^-.

Theorem 2. Consider the system in the positive electrode (III.4)-(III.6) and the state observer (III.26)-(III.28) with the designed gains (III.24) and (III.25). For any initial condition under assumptions, if $\lambda \geq -\frac{1}{4}$, then the origin of the estimation error system (III.29)-(III.31) will be exponentially stable, which means the designed observer (III.26)-(III.28) converges exponentially to the system (III.4)-(III.6).

D. Electrolyte observer for separator

An observer for the normalized system within the separator (III.7)-(III.9) is designed as follows:

$$\frac{\partial \hat{c}_{\mathrm{e}}^{\mathrm{sep}}}{\partial t}(t,x) = \frac{\partial^2 \hat{c}_{\mathrm{e}}^{\mathrm{sep}}}{\partial x^2}(t,x) + p_1(x)\tilde{c}_{\mathrm{e}}^{\mathrm{sep}}(t,0^{\mathrm{sep}}), \tag{III.33}$$

$$\frac{\partial \hat{c}_{\mathrm{e}}^{\mathrm{sep}}}{\partial x}(t,0^{\mathrm{sep}}) = \frac{-L^-\hat{c}_{\mathrm{e}}^-(t,0^{\mathrm{sep}})}{P^*} - p_{10}\tilde{c}_{\mathrm{e}}^{\mathrm{sep}}(t,0^{\mathrm{sep}}), \tag{III.34}$$

$$\frac{\partial \hat{c}_{\mathrm{e}}^{\mathrm{sep}}}{\partial x}(t,1^{\mathrm{sep}}) = \frac{L^+\hat{c}_{\mathrm{e}}^+(t,1^{\mathrm{sep}})}{L^{\mathrm{sep}} - P^*}, \tag{III.35}$$

where $\tilde{c}_{\mathrm{e}}^{\mathrm{sep}}(t,x) = c_{\mathrm{e}}^{\mathrm{sep}}(t,x) - \hat{c}_{\mathrm{e}}^{\mathrm{sep}}(t,x)$. These observers are cascaded, allowing $c_{\mathrm{e}}^{\mathrm{sep}}(t,0^{\mathrm{sep}}) = c_{\mathrm{e}}^{\mathrm{sep}}(t,L^-)$ to be obtained from the estimation results of the negative electrode observer.

Authorized licensed use limited to: Texas Tech University. Downloaded on March 19,2025 at 15:08:22 UTC from IEEE Xplore. Restrictions apply.

The dynamics of the state error $\tilde{c}_{\mathrm{e}}^{\mathrm{sep}}(t,x)$ are obtained as:

$$\frac{\partial \tilde{c}_{\mathrm{e}}^{\mathrm{sep}}}{\partial t}(t,x) = \frac{\partial^2 \tilde{c}_{\mathrm{e}}^{\mathrm{sep}}}{\partial x^2}(t,x) + p_1(x)\tilde{c}_{\mathrm{e}}^{\mathrm{sep}}(t,0), \tag{III.36}$$

$$\frac{\partial \tilde{c}_{\mathrm{e}}^{\mathrm{sep}}}{\partial x}(t,0) = \frac{-L^+\tilde{c}_{\mathrm{e}}^{+}(t,1^{\mathrm{sep}})}{P^*} - p_{10}\tilde{c}_{\mathrm{e}}^{\mathrm{sep}}(t,0), \tag{III.37}$$

$$\frac{\partial \tilde{c}_{\mathrm{e}}^{\mathrm{sep}}}{\partial x}(t,1) = \frac{-L^+\tilde{c}_{\mathrm{e}}^{+}(t,1^{\mathrm{sep}})}{L^{\mathrm{sep}} - P^*}, \tag{III.38}$$

where

$$p_{10} = q^- - \frac{\alpha}{2}, \tag{III.39}$$

and $p_1(x)$ is given in (III.24). Subsequently, with the following invertible transformation:

$$\tilde{c}_{\mathrm{e}}^{\mathrm{sep}}(t,x) = \tilde{w}(t,x) - \int_0^x p(x,y)\tilde{w}(t,y)dy, \tag{III.40}$$

and the proposed gains, the state error system (III.36)-(III.38), will be exponentially stable.

Theorem 3. Consider the normalized system in the separator (III.7)-(III.9), the proposed state observer (III.33)-(III.35), and its gains (III.24) and (III.39). For any initial condition under assumptions, if $\lambda \geq -\frac{1}{4}$, then the origin of the error system (III.36)-(III.38) is exponentially stable, which means the designed observer (III.33)-(III.35) converges exponentially to the system (III.7)-(III.9).

IV. Simulation

The simulation is conducted on a $LiFePO_4$ battery cell with a rated capacity of 2.3 Ah. The simulation was performed using MATLAB on a MacBook Pro equipped with an Apple M2 CPU and 8 GB of RAM. The temperature is assumed to remain constant at $T = 298$ K. The electrochemical parameters of the battery model are adopted from Table 1 in [14]. The UDDS current profile [7], shown in Fig. 3, is employed as the system's input.

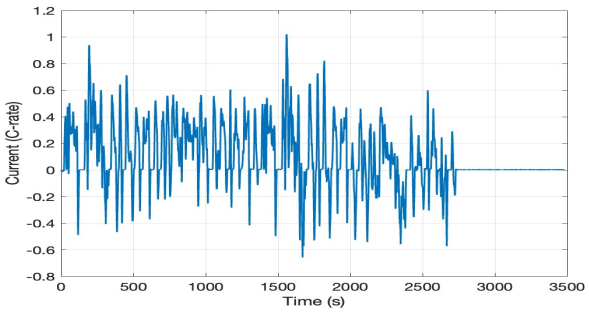

Fig. 3: UDDS current profile

This simulation utilizes the forward finite difference method. The initial conditions for the original systems are set at 2000 mol/m^3, while for the observers, they are set at 1950 mol/m^3. The electrolyte lithium ion concentration in the negative electrode and its estimation based on the proposed observer are depicted in Fig. 4 and Fig. 5, respectively. The estimation error for the negative electrode $\tilde{c}_e^-(t,x)$, is illustrated in Fig. 6. Initially, there is a large error, but it quickly diminishes, converging to zero over time. The

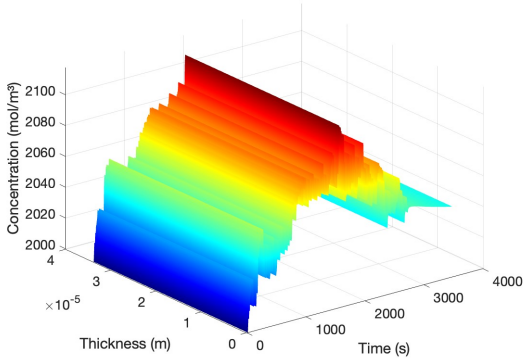

Fig. 4: Electrolyte lithium ion concentration in the negative electrode $c_e^-(t,x)$

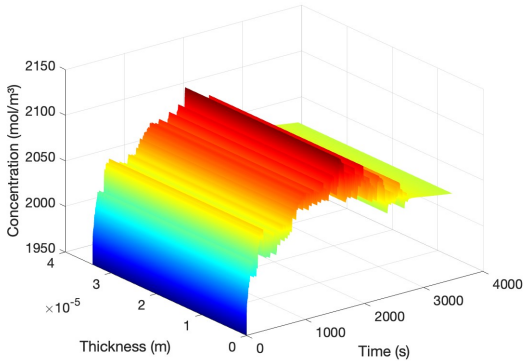

Fig. 5: Estimation of electrolyte lithium ion concentration in the negative electrode $\hat{c}_e^-(t,x)$

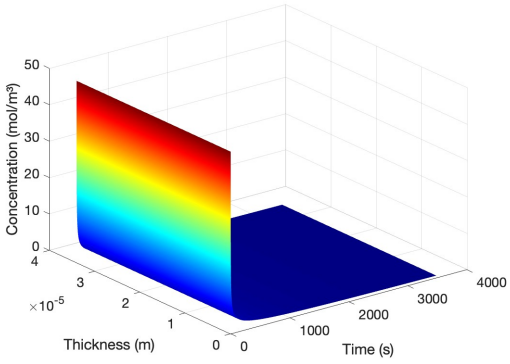

Fig. 6: Estimation error of electrolyte lithium ion concentration in the negative electrode $\tilde{c}_e^-(t,x)$

electrolyte lithium ion concentration in the positive electrode and its estimation through the proposed observer are plotted in Fig. 7 and Fig. 8, respectively. Fig. (9) depicts the estimation error for the positive electrode $\tilde{c}_e^+(t,x)$. Initially, a substantial error is observed, which rapidly decreases over time. Simulations of the separator are not included in this version due to its quasi-linear behavior, which mimics the trend shown in Fig 2.

Authorized licensed use limited to: Texas Tech University. Downloaded on March 19,2025 at 15:08:22 UTC from IEEE Xplore. Restrictions apply.

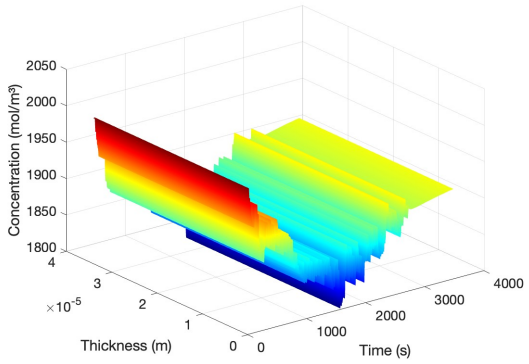

Fig. 7: Electrolyte lithium ion concentration in the positive electrode $c_e^+(t,x)$

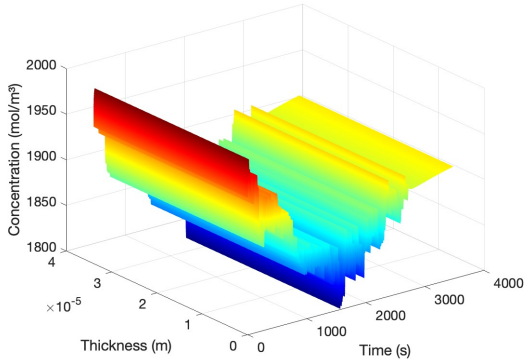

Fig. 8: Estimation of electrolyte lithium ion concentration in the positive electrode $\hat{c}_e^+(t,x)$

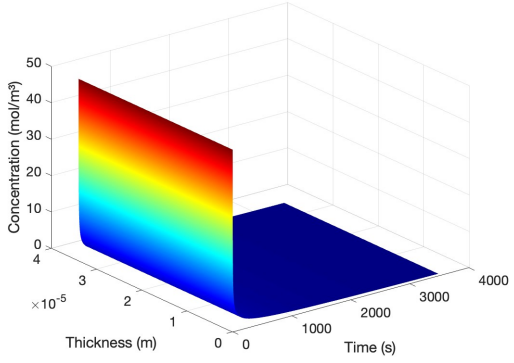

Fig. 9: Estimation error of electrolyte lithium ion concentration in the positive electrode $\tilde{c}_e^+(t,x)$

V. Conclusion

This paper proposes a provably convergent state observer for electrolyte concentration in different regions of lithium-ion batteries, utilizing a PDE backstepping approach. The SPMe model used enables the proposed observer to balance accuracy and computational efficiency. Simulation results confirm that the estimation error converges as expected. In this study, modified boundary conditions are employed to design the observers, but future work will focus on utilizing coupled boundary conditions.

For the design of observers, concentration data at the terminal boundaries is required. Based on the reverse sensitivity analysis results in [8], electrolyte resistance is identified as the most suitable measurement for $LiFePO_4$ battery cells. Developing the proposed observer into an adaptive model to incorporate aging effects on specific parameters is another area for future research. Additionally, exploring working conditions beyond the UDDS current profile and considering robustness to enhance the proposed method are potential avenues for further study. Experimental studies can also be conducted to validate the proposed scheme.

References

[1] Sara Sepasiahooyi and Shu-Xia Tang. Sensitivity analysis of lithium-ion battery soh indicators: An analytical study. In *2024 American Control Conference (ACC)*, pages 1971–1976. IEEE, 2024.

[2] Sadiqa Jafari, Yung-Cheol Byun, and Seokjun Ko. A Novel Approach for Predicting Remaining Useful Life and Capacity Fade in Lithium-Ion Batteries using Hybrid Machine Learning. *IEEE Access*, 2023.

[3] Vahid Safavi, Najmeh Bazmohammadi, Juan C Vasquez, and Josep M Guerrero. Battery state-of-health estimation: A step towards battery digital twins. *Electronics*, 13(3):587, 2024.

[4] Sara Sepasiahooyi and Farzaneh Abdollahi. Fault detection of new and aged lithium-ion battery cells in electric vehicles. *Green Energy and Intelligent Transportation*, page 100165, 2024.

[5] Scott J Moura, Nalin A Chaturvedi, and Miroslav Krstić. Adaptive partial differential equation observer for battery state-of-charge/state-of-health estimation via an electrochemical model. *Journal of Dynamic Systems, Measurement, and Control*, 136(1):011–015, 2014.

[6] Shu-Xia Tang, Leobardo Camacho-Solorio, Yebin Wang, and Miroslav Krstic. State-of-charge estimation from a thermal–electrochemical model of lithium-ion batteries. *Automatica*, 83:206–219, 2017.

[7] Scott J Moura, Federico B Argomedo, Reinhardt Klein, Anahita Mirtabatabaei, and Miroslav Krstic. Battery state estimation for a single particle model with electrolyte dynamics. *IEEE Transactions on Control Systems Technology*, 25(2):453–468, 2016.

[8] Sara Sepasiahooyi and Shu-Xia Tang. Enhanced battery state estimation: Part 2 – reverse sensitivity analysis and electrode lithium-ion observer. In *Conference on Decision and Control*. IEEE, 2024.

[9] Shanthan K Padisala, Sara Sattarzadeh, and Satadru Dey. Reduced and reformulated electrochemical model-based detection and isolation of electrode-level faults in lithium-ion battery cells. *IFAC-PapersOnLine*, 55(37):734–739, 2022.

[10] Jianing Xu, Tiansi Wang, Lei Pei, Shitong Mao, and Chunbo Zhu. Parameter identification of electrolyte decomposition state in lithium-ion batteries based on a reduced pseudo two-dimensional model with padé approximation. *Journal of Power Sources*, 460:228093, 2020.

[11] Alexandros Ch Lazanas and Mamas I Prodromidis. Electrochemical impedance spectroscopy a tutorial. *ACS Measurement Science Au*, 2023.

[12] Kaixin Cui, Shu-Xia Tang, Yuan Huang, Hao Yu, and Dawei Shi. Event-triggered active disturbance rejection control for a class of networked systems with unmatched uncertainties: Theoretic and experimental results. *Control Engineering Practice*, 115:104907, 2021.

[13] Bhathiya Rathnayake, Mamadou Diagne, Nicolás Espitia, and Iasson Karafyllis. Observer-based event-triggered boundary control of a class of reaction–diffusion pdes. *IEEE Transactions on Automatic Control*, 67(6):2905–2917, 2021.

[14] Shifei Yuan, Lei Jiang, Chengliang Yin, Hongjie Wu, and Xi Zhang. A transfer function type of simplified electrochemical model with modified boundary conditions and padé approximation for li-ion battery: Part 1. lithium concentration estimation. *Journal of Power Sources*, 352:245–257, 2017.

Authorized licensed use limited to: Texas Tech University. Downloaded on March 19,2025 at 15:08:22 UTC from IEEE Xplore. Restrictions apply.